

A Yeast Purification System for Human Translation Initiation Factors eIF2 and eIF2B ϵ and Their Use in the Diagnosis of CACH/VWM Disease

Rogério A. de Almeida¹, Anne Fogli^{2,3,4}, Marina Gaillard², Gert C. Scheper^{5‡}, Odile Boesflug-Tanguy^{6,7,8}, Graham D. Pavitt^{1*}

1 Faculty of Life Sciences, The University of Manchester, Manchester, United Kingdom, **2** Laboratoire GReD (Génétique, Reproduction et Développement), Faculté de Médecine, INSERM U1103 CNRS 6293, Clermont-Ferrand, France, **3** Université de Clermont, UFR Médecine, Clermont-Ferrand, France, **4** Centre Hospitalier Universitaire de Clermont-Ferrand, Service de Biochimie Médicale et Biologie Moléculaire, Clermont-Ferrand, France, **5** Department of Pediatrics, VU University Medical Centre, Amsterdam, The Netherlands, **6** INSERM U676, Hôpital Robert Debré, Paris, France, **7** Université Paris Diderot, Sorbonne Cité, UMR U676, Paris, France, **8** APHP, Hôpital Robert Debré, Pediatric Neurology and Metabolic Diseases, Reference Center for Leukodystrophies, Paris, France

Abstract

Recessive inherited mutations in any of five subunits of the general protein synthesis factor eIF2B are responsible for a white matter neurodegenerative disease with a large clinical spectrum. The classical form is called Childhood Ataxia with CNS hypomyelination (CACH) or Vanishing White Matter Leukoencephalopathy (VWM). eIF2B-related disorders affect glial cells, despite the fact that eIF2B is a ubiquitous protein that functions as a guanine-nucleotide exchange factor (GEF) for its partner protein eIF2 in the translation initiation process in all eukaryotic cells. Decreased eIF2B activity measured by a GEF assay in patients' immortalised lymphocytic cells provides a biochemical diagnostic assay but is limited by the availability of eIF2 protein, which is classically purified from a mammalian cell source by column chromatography. Here we describe the generation of a recombinant expression system to produce purified human eIF2 from yeast cells. We demonstrate that human eIF2 can function in yeast cells in place of the equivalent yeast factor. We purify human eIF2 and the C-terminal domain of human eIF2B ϵ using affinity chromatography from engineered yeast cells and find that both function in a GEF assay: the first demonstration that this human eIF2B ϵ domain has GEF function. We show that CACH/VWM mutations within this domain reduce its activity. Finally we demonstrate that the recombinant eIF2 functions similarly to eIF2 purified from rat liver in GEF assays with CACH/VWM eIF2B-mutated patient derived lymphocytic cells.

Citation: de Almeida RA, Fogli A, Gaillard M, Scheper GC, Boesflug-Tanguy O, et al. (2013) A Yeast Purification System for Human Translation Initiation Factors eIF2 and eIF2B ϵ and Their Use in the Diagnosis of CACH/VWM Disease. PLoS ONE 8(1): e53958. doi:10.1371/journal.pone.0053958

Editor: Eric Jan, University of British Columbia, Canada

Received: October 4, 2012; **Accepted:** December 4, 2012; **Published:** January 15, 2013

Copyright: © 2013 de Almeida et al. This is an open-access article distributed under the terms of the Creative Commons Attribution License, which permits unrestricted use, distribution, and reproduction in any medium, provided the original author and source are credited.

Funding: European Leukodystrophy association (ELA) ela-asso.com; grant: ELA 2009-03415 to GDP, and The European Union EU-FP7 Health project Leukotreat 241622; <http://www.leukotreat.eu/>. The funders had no role in study design, data collection and analysis, decision to publish, or preparation of the manuscript.

Competing Interests: Dr. Scheper is an employee Crucell Holland BV. There are no patents, products in development or marketed products to declare. This does not alter the authors' adherence to all the PLOS ONE policies on sharing data and materials, as detailed online in the guide for authors.

* E-mail: graham.pavitt@manchester.ac.uk

‡ Current address: Crucell Holland BV, Leiden, The Netherlands

Introduction

Childhood Ataxia with CNS hypomyelination (CACH) or Vanishing White Matter Leukoencephalopathy (VWM) (OMIM #603896) was described in the 1990s [1,2]. It is a fatal childhood onset white matter disease with a chronic progressive course exacerbated by acute episodes [3,4]. Inherited mutations in any of the five genes encoding subunits of the general protein synthesis initiation factor eIF2B (*EIF2B1-5*) cause CACH/VWM [3,5]. The subsequent description of a large clinical spectrum of the disease from neonatal to adult onset or even asymptomatic forms led to the concept of eIF2B-related disorders that are recognized by peculiar magnetic resonance imaging (MRI) abnormalities [6]. Well over 100 different, mainly missense, mutations have been presently reported [4]. Their consequences on the eIF2B complex have been demonstrated in yeast and in humans [7,8,9]. Abnormalities in glial cell development have been suggested by studies of patient samples [10,11,12,13,14,15,16] and studies of a

mouse model [17]. One recent suggested explanation is that altered expression of splicing regulatory factors in eIF2B mutated glial cells may cause altered splicing regulation of the important myelin proteins PLP and DM20 [18]. However many aspects of the disease are still not understood and no current therapy is available.

eIF2B is well established as a key regulated general translation initiation factor. It functions as a guanine nucleotide exchange factor (GEF) to accelerate the dissociation of GDP from its substrate eIF2•GDP in the first step of translation initiation to form eIF2•GTP [19]. This complex then binds to initiator methionyl tRNA (Met-tRNA_i^{Met}) to deliver it to 40S ribosomes in a reaction that is stimulated by several other translation factors and is required for each translation initiation event on almost all mRNAs [20,21]. During the initiation cycle eIF2-bound GTP is hydrolysed to GDP to inactivate eIF2 and reset the system. eIF2B is regulated by cellular stresses facilitating translational control in a wide variety of settings. Most widely studied is the activation of eIF2 α

kinases that phosphorylate eIF2 on its alpha subunit at Ser51 [22]. This phosphorylation reaction converts eIF2 from substrate to inhibitor of eIF2B. When phosphorylated at Ser51, eIF2 binds with higher affinity to eIF2B, but without undergoing nucleotide exchange [19]. Genetic and biochemical studies using eIF2B from yeast identified mutations in three subunits of eIF2B (eIF2B $\alpha\beta\delta$) that disrupt this regulation and define a potential regulatory interface between eIF2 and eIF2B that is critical for regulation [23]. Subsequent experiments verified that equivalent mutations in mammalian eIF2B also disrupt eIF2B regulation confirming conservation of this regulatory mechanism [24,25].

eIF2B activity is measured by a GEF assay that was first established in the 1980s [26,27]. eIF2 forms a stable complex with GDP in the presence of physiological concentrations of Mg²⁺ ions. It requires significant amounts of eIF2 protein purified from rat liver, rabbit reticulocytes or mammalian cell lysates by rounds of conventional column chromatography [27,28]. Pure eIF2 mixed with radiolabelled GDP in the presence of Mg²⁺ acts as a substrate and eIF2B is added along with excess unlabelled nucleotide. eIF2B promotes release of labelled GDP and this is assayed by monitoring the progressive decline in labelled eIF2 captured on protein-binding filters. Two versions of the assay have been used; employing either purified eIF2B proteins or extracts from cultured cells. Both formats of the assay have been useful in defining that the largest subunit of eIF2B (eIF2B ϵ) is the only one that possesses GEF activity, and that this activity is enhanced by complex formation with the other four subunits. Catalytic activity has been shown for yeast, drosophila and mammalian proteins [29,30,31]. In addition experiments using purified yeast proteins showed that the C-terminal ~200 amino acids contained all the elements necessary for minimal exchange function. This region was termed the catalytic domain ϵ cat [32,33].

The cell extract format of the assay has been used to assess eIF2B activity in immortalised lymphocytic cells isolated from blood samples of CACH/VWM patients [9,10,34]. This provides a biochemical diagnostic assay to complement MRI and genetic analyses. The adoption of this GEF assay for diagnostic purposes is limited by the availability of purified eIF2 protein. We, and others, have previously developed a yeast cell expression system to overexpress and purify epitope tagged yeast eIF2, which was subsequently used for *in vitro* studies [29,35]. Generating recombinant systems for mammalian eIF2 has proved challenging because eIF2 possesses three different subunits in a 1:1:1 complex, and because popular expression host cells, including *Escherichia coli*, appear refractory to expressing significant amounts of the gamma subunit. We therefore decided to develop a recombinant yeast cell system to purify active human eIF2 protein.

Results and Discussion

Human eIF2 Subunits can Complement the Function of the Equivalent Yeast Gene

The translation initiation factor eIF2 performs critical roles in the initiation and control of protein synthesis in eukaryotic cells. eIF2 is composed of three non-identical subunits and must interact with GDP, GTP, Met-tRNA^{Met}, eIF3, eIF5, eIF2B and 40S ribosomes to perform its functions [35,36,37] as well several eIF2 α protein kinases for regulation. eIF2 has an archaeal homologue, but is not found in eubacteria [38]. eIF2 subunits are highly conserved between yeast and mammals, including humans (Figure 1A). We decided to develop a yeast system as an expression vehicle for human eIF2 (*heIF2*). As a first step we obtained cDNA clones and subcloned them into yeast expression vectors, under the control of conditional (galactose carbon source

inducible) yeast promoters and bearing short terminal epitope tags (Figure 1B and Materials and Methods). Each yeast eIF2 gene is essential (*SUI2*, *SUI3*, and *GCD11* encoding eIF2 α - γ respectively). Strains bearing individual gene deletions covered by a plasmid copy of the yeast gene were used to assess the function of the human expression clones. Each human vector was introduced into its corresponding yeast deletion strain by transformation and plasmid shuffling was used to evict the covering plasmid. We found that plasmids bearing *EIF2S1* encoding *heIF2 α* complemented a *sui2 Δ* (Figure 1C, compare lanes 2 and 3 with lane 1) and grew as well as wild type yeast. Similarly plasmids bearing *EIF2S2* encoding *heIF2 β* complemented *sui3 Δ* (Figure 1C, compare lanes 5 and 6 with lane 4). However our initial *EIF2S3* plasmids (encoding *heIF2 γ*) could not complement *gcd11 Δ* (data not shown). As *EIF2S3* contains a significant number of codons rarely used in yeast we obtained a commercially synthesised yeast-codon-optimized clone and subcloned this into a similar compatible yeast expression plasmid. This could complement the *gcd11 Δ* strain, but the resulting strain grew poorly (Figure 1C, lane 8). Western blotting confirmed both deletion of endogenous yeast genes and expression of the corresponding *heIF2* subunits (Figure 1D). Because eIF2 functions as a heterotrimer, in these complemented cells heterologous eIF2 complexes should form, each with one human and two yeast subunits.

We were concerned by the slow growth of the *EIF2S3* complemented strain (Figure 1C, lane 8), as this may indicate that the codon-optimized cDNA is not fully functional. Several explanations are possible. Firstly, *heIF2 γ* may not be expressed at a high enough level to form sufficient eIF2 complexes for rapid growth. Expression of *heIF2 γ* did not alter the expression levels of the yeast α and β subunits (Figure 1D). We observed that different *EIF2S3* transformants grew at different rates. When the expression level of *heIF2 γ* was examined in a selection of these cells, we consistently found that transformants expressing the highest *heIF2 γ* levels grew more slowly than those with lower expression (Figure 2A and data not shown). These results are therefore more consistent with the idea that the slow-growth phenotype is related to excess levels of *heIF2 γ* . Excess free *heIF2 γ* may bind to and sequester one or more interacting factors into non- or partially functional complexes. This second idea however is unlikely as the slow-growth phenotype is recessive. *heIF2 γ* is only slow growing in the absence of yeast *GCD11* (Figure 2B and data not shown).

Because eIF2 γ is the 'core' subunit that binds to both eIF2 α and β [38], excess *heIF2 γ* may form some $\alpha\gamma$ or $\beta\gamma$ complexes and thereby reduce the level of full $\alpha\beta\gamma$ complexes. If so, then reducing excess *heIF2 γ* may ameliorate complex disruption and improve growth as observed. Alternatively, because eIF2 must interact with many yeast factors including translation factors (eIF2B, eIF5, eIF3) Met-tRNA^{Met} and 40S ribosomes, *heIF2 γ* may not interact effectively with one or more of these. We assessed whether transforming the *heIF2 γ* strain with additional copies of yeast eIF2-interacting factors could complement the growth phenotype by mass action. A panel of high copy plasmids expressing tRNA^{Met} or combinations of subunits of eIF2B, eIF3 or eIF5 was transformed into the *gcd11 Δ* strain expressing *heIF2 γ* (see Methods for plasmids assessed). Only excess eIF5 reproducibly suppressed the slow-growth phenotype (Figure 2B and data not shown). Western blotting confirmed that slow-growth suppression in these cells was not caused by reduced *heIF2 γ* expression (Figure 2C). eIF5 interacts with both eIF2 β and γ [36] as part of the multifactor complex [39], 43S pre-initiation complex and free eIF2 [40,41]. It has GTPase acceleration and GDP-dissociation inhibitor functions [42]. While not conclusive, perhaps impaired contact between the hybrid eIF2 and yeast eIF5 affects eIF2 or

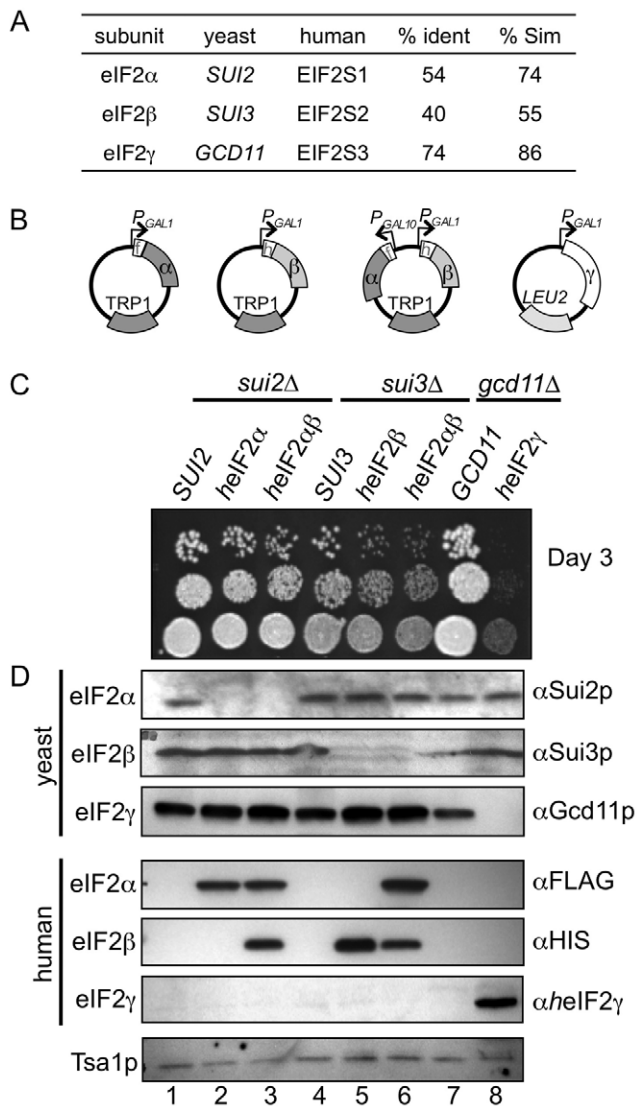


Figure 1. Individual *heIF2* cDNAs replace the function of the corresponding yeast gene. A. Table comparing yeast and human eIF2 subunit proteins. B. Cartoon depiction of plasmids pAV1907 (α), pAV1901 (β), pAV1905 (α,β) and pAV1970 (γ), respectively that express the indicated human eIF2 subunits from either *GAL1* or *GAL10* promoters. N-terminal his₆ (h) and flag (f) epitope tags are also shown. C. Growth of yeast strains following plasmid shuffling on YPGal medium and D. Western blotting of the same strains using the antibodies indicated. Tsa1p is shown as a loading control. Strains shown in lanes 1–8 are: GP3001, GP5108, GP5109, GP5010, GP5110, GP5111, GP5012, GP5613.

doi:10.1371/journal.pone.0053958.g001

eIF5 function and that this could be suppressed by mass action. For example excess eIF5 may prevent its premature loss from initiating ribosomes. Alternatively it may stabilise eIF2 $\beta\gamma$ interactions within the eIF2 complex. Because eIF5 interacts with many initiation factors, several other explanations where the suppressing effect is less direct are also possible to envisage. As the main focus of our study was to generate an expression system to purify active human eIF2, we decided not to investigate these heteromeric yeast-human hybrid complexes further and instead focussed on co-expression of all three human subunits.

Co-expression of All Three *heIF2* Subunits Complements a Triple Yeast eIF2 Gene Deletion Strain

Dever and colleagues recently reported construction of a triple eIF2 gene deletion yeast strain complemented by a single plasmid expressing the yeast genes [43]. To assess if co-expression of all three *heIF2* subunits could completely replace the yeast factor, we modified this strain to create a *trp1* selectable marker (see Materials and Methods) and transformed in two *heIF2* plasmids. One plasmid co-expressed both *heIF2* $\alpha\beta$ and a second plasmid expressed *heIF2* γ . Plasmid shuffling with FOA generated yeast strains entirely supported by *heIF2* (Figure 3A, lower panel). As expected, growth was carbon source dependent. When expression of *heIF2* genes from *P_{GAL}* promoters was repressed by glucose, *heIF2*-dependent strains failed to grow (Figure 3A, upper panel). Western blotting confirmed that the yeast genes had been deleted and that higher expression of *heIF2* conferred a slower rate of growth (Figure 3B). In conclusion, our *heIF2* is functional and can replace the yeast protein *in vivo*.

Purification of Human eIF2 and Catalytic Domains

Because we appended small epitope tags to each *heIF2* subunit, we used affinity chromatography to purify the protein complex. We employed a yeast strain deleted for the only yeast eIF2 kinase *GCN2*. This means that unlike the proteins purified from mammalian sources, our recombinant eIF2 is homogeneously unphosphorylated at the key regulatory site, Ser 51 of the alpha subunit. Purification by a single step using Flag M2 affinity resin to bind *heIF2* α , or a single nickel agarose step to bind *heIF2* β was not sufficient to purify *heIF2* (Figure 4A). The single step Flag affinity purification recovered a mixture of $\alpha\beta\gamma$ trimers, excess eIF2 α and residual contaminating proteins (Figure 4A lanes 2–7). Similarly a single-step his₆ purification captured a mixture of $\alpha\beta\gamma$ trimers and excess eIF2 β (Figure 4A, lanes 8–12 and 4B, lanes 2–6). These results are consistent with the known structure of the archaeal homologue of eIF2, aIF2 $\alpha\beta\gamma$ where both aIF2 α and β each separately bind to aIF2 γ [38] and with the idea that expression of *heIF2* γ in our cells is limiting, so that excess free *heIF2* α and β subunits are formed. We therefore adopted a two-step purification strategy employing nickel agarose, followed by Flag resin (Figure 4B) to purify heterotrimeric eIF2 free from excess α and β subunits (Figure 4B, lane 11). Because eIF2 γ expression levels were limiting in our system we transformed in a second plasmid to boost the amounts of the full eIF2 complex. With this strategy we obtained eIF2 that was approximately 90% pure (Figure 4C).

We wished to assess nucleotide binding and exchange with our *heIF2* protein. The nucleotide exchange factor eIF2B is specific for eIF2. eIF2B is composed of five distinct subunits. However previous work has shown that the largest subunit alone retains catalytic function and studies in yeast showed that the carboxy terminal domain alone (yeast residues 518–712) is the catalytic domain, termed ϵ cat [32]. Subsequently, deletion of residues 549–596 within human eIF2B ϵ resulted in a protein that could form eIF2B complexes, but had no GEF activity *in vitro* showing this region is critical for human eIF2B GEF function [8]. In addition X-ray crystallographic structure determination has shown that the human equivalent domain adopts the same stacked, paired α -helical structure as the yeast ϵ cat [33,44]. We therefore predicted that a construct bearing the equivalent residues of human eIF2B ϵ , residues 533–721 would comprise the human eIF2B catalytic domain (*h2B ϵ cat*). A yeast codon-optimized *h2B ϵ cat* cDNA was synthesized and expressed with tandem Flag and polyhistidine tags from a galactose inducible promoter vector in a suitable yeast strain host and the same purification scheme devised for *heIF2* was

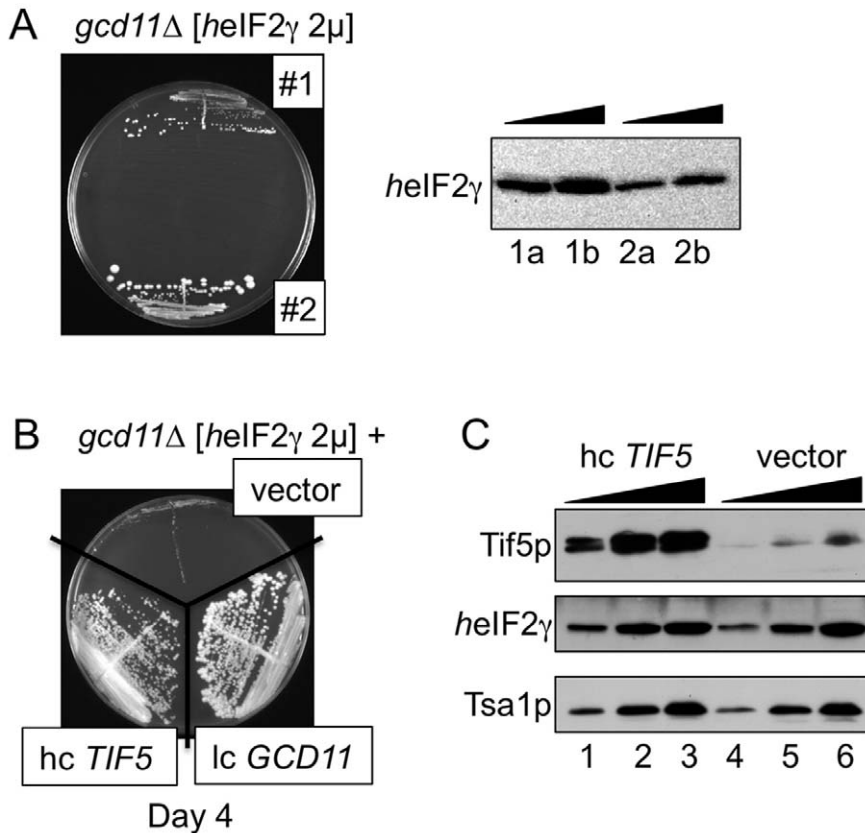


Figure 2. Reducing *heIF2γ* expression levels or overexpressing eIF5 suppress the slow growth phenotype conferred by *heIF2γ* overexpression. A. Reciprocal variation in growth and expression level of *heIF2γ* in 5-FOA resistant colonies (#1 and #2) following transformation of pAV1970 into GP5012. Left, growth on YPGal medium (Day 7). Right, anti-*heIF2γ* western blot from liquid cultures of the same transformants: lanes a and b 1x and 2x loadings, respectively. B. Transformant #1 (GP5613) was transformed plasmids pRS426, pAV1280 or pAV2015 to make strains GP5744 (vector), GP5755 (*GCD11*) and GP5758 (hc *TIF5*) respectively and grown on YPGal medium (Day 4). C. western blots showing increasing loadings (0.5X, 1X, 2X) of cell extracts from GP5758 (lanes 1–3) and GP5744 (lanes 4–6) with indicated antibodies. Tsa1p is shown as a loading control. doi:10.1371/journal.pone.0053958.g002

used (Figure 4C). To assess the functions of purified *heIF2* and *h2Becat*, we set up a standard nucleotide exchange assay with radiolabelled GDP (see Materials and Methods). In the absence of eIF2B, but in the presence of excess unlabelled GDP, *heIF2* bound [³H]GDP at 10–30°C with MgCl₂ from 0.2–2 mM. This indicates that the nucleotide binding function of *heIF2* is intact. When *h2Becat* was added, this stimulated release of [³H]GDP with first order kinetics (Figure 4C). This confirms that nucleotide binding to eIF2 is reversible and that residues 533–721 of human eIF2Bε contains the catalytic domain.

Catalytic Domain CACH/VWM Mutants have Reduced GEF Activity

As stated in the introduction, mutations in eIF2B cause a genetic disease. Mutations have been found in all five subunits, including several within the catalytic domain. Catalytic domain mutations include missense alleles: P604S [45], I649T [46], E650K [47], M608I [48] and W684S [49] and small deletions: Δ610–613 [9] Δ666–672 [47]. In all patients reported thus far, these alleles occur as compound heterozygotes with other mutations contributing to the disease pathology and the measured eIF2B activity from patient cells. Using a mammalian cell expression system, the Proud laboratory has pioneered *in vitro* biochemical analyses of eIF2B CACH/VWM mutants. Typically HEK293 cells are transformed with vectors overexpressing all five

subunits of eIF2B, which are affinity purified and the resulting complexes analysed for complex formation and GEF activity. For example when analysed as part of 5-subunit complex W628R reduced activity to ~20% [8], I649T to ~40% and E650K to ~30% of wild type [49]. The latter two also apparently reduced association with the alpha (and possibly delta) subunits of eIF2B [49] indicating possible reduced complex integrity that could contribute to reduced activity. The Δ610–613 mutant dramatically reduced expression or subunit stability and activity to 25% [9].

To further test our recombinant *heIF2* and *h2Becat*, we introduced several mutations into our *h2Becat* expression vector and purified these to homogeneity (Figure 5). We included mutations that had been analysed as part of 5-subunit eIF2B complexes (W628R, I649T and E650K) as well as mutations not analysed previously (P604S and Δ666–672). All mutant forms significantly reduced GEF activity (Figure 5), validating that our *heIF2* and *h2Becat* behave as expected. It was perhaps surprising that the Δ666–672 mutant had only a modest reduction in activity, when compared with missense mutations that might be predicted to have a smaller impact on the overall structure. Examining the locations of the mutated residues on the human catalytic domain structure [33,44] suggests that most of the missense mutations affect residues predominantly buried internally within the structure. Macromolecular modelling of the impact of the Δ666–672 mutant, suggests that the normal domain fold can be adopted, but

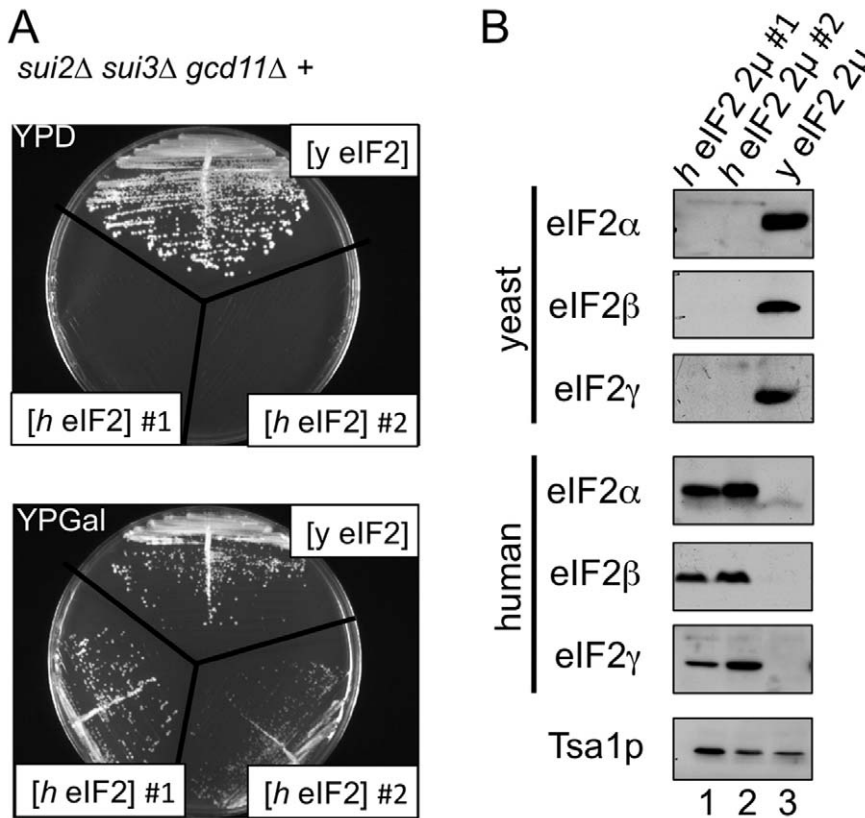


Figure 3. All three *heIF2* cDNAs can replace yeast eIF2 in a triple deletion strain. A. Growth of yeast strains GP6124 (yefF2), GP6461 (*heIF2* #1), GP6462 (*heIF2* #2) on glucose containing YPD medium (represses *heIF2* expression; top) and galactose YPGal medium (bottom; *heIF2* expression inducing conditions). B. Western blots of cell extracts from the same strains grown in YPGal medium. doi:10.1371/journal.pone.0053958.g003

that there is local disruption of part of one α -helix only (data not shown). The affected helix does not contribute to the surface regions of ϵ cat identified previously as critical for direct eIF2 binding and activity [50]. This observation appears to fit with the modest reduction in GEF activity observed for *h2B ϵ cat*, but does not rule out that it may have a more significant defect *in vivo* in the context of the full five subunit protein complex.

heIF2 Functions in GEF Assays with Extracts from Patient-derived Cells

Extracts from patient-derived cells have been used as a source of eIF2B to provide biochemical diagnosis for eIF2B related disorders [10,34]. To assess whether our *heIF2* would perform as a substrate in GEF assays with patient cells, we performed assays with lymphoblastoid cell line extracts from 18 CACH/VWM patients and compared the results to those obtained previously with the rat eIF2 substrate classically used for this diagnostic assay (Table 1). Our panel of cell lines included mutations in four of the five eIF2B subunits and those previously shown to have a range of disease severity from severe, early onset to classical/mild forms of disease [34].

Firstly, we observed a decreased GEF activity ($\leq 87.2\%$) using the *heIF2* substrate for the patient cell lines which exhibited a decreased GEF activity under the previously described diagnostic threshold (77.5%) using rat eIF2 as substrate [34]. The GEF activity values using the *heIF2* substrate are marginally higher and show more variability (with a mean SD = 9.1% using *heIF2* in comparison to 4.8% using rat eIF2 with a correlation factor

between the two assays of $r = 0.78$). The disease-diagnostic threshold used with this substrate should therefore be revised from 77.5% to 89.9%. Using this new value, the diagnostic impact of the GEF assay is identical to the assay using rat eIF2: the patients with GEF activity $< 77.5\%$ with rat eIF2 exacerbated also a GEF activity $< 89.9\%$ with yeast *heIF2* (Table 1). There are several possible reasons that may explain the observed minor difference between the two sources of eIF2. Firstly, there are minor sequence variations between the two species. Secondly there may be differences in post-translational modifications between the two preparations. For example, we assume that eIF2 from rat liver will be partially phosphorylated at ser51 by endogenous eIF2 alpha kinases, while *heIF2* from yeast is unphosphorylated. Phosphorylated eIF2 inhibits eIF2B reducing the observed activity. Specific mutations in the α , β and δ subunits alter the sensitivity of eIF2B to inhibition by phosphorylated eIF2 [23,24,25]. However it is not yet known whether disease-causing mutations alter eIF2B sensitivity to eIF2 phosphorylation.

Cells from two patients tested here (432-1 and 1074-1) exhibited normal GEF activity using the rat eIF2 substrate. Here lower GEF activity was found with the *heIF2* substrate, taking patient 432-1 just below the proposed diagnostic threshold (Table 1). A recent report also identified two severe CACH/VWM patients with eIF2B mutations, but no apparent defect in eIF2B activity [49]. However the eIF2B GEF activity for those patients was measured only in primary fibroblasts. Further studies are needed to assess the diagnostic value of measuring eIF2B GEF activity in fibroblasts. Discrepancies have been previously reported between measuring

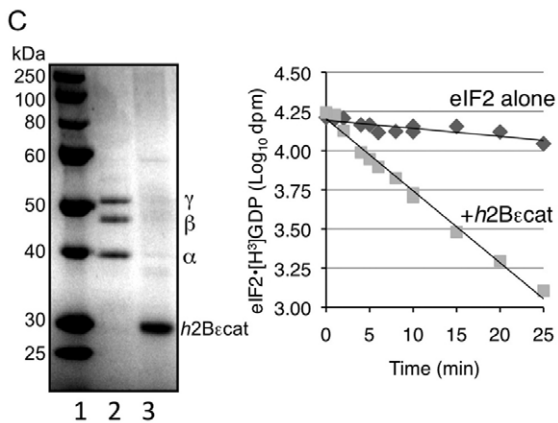
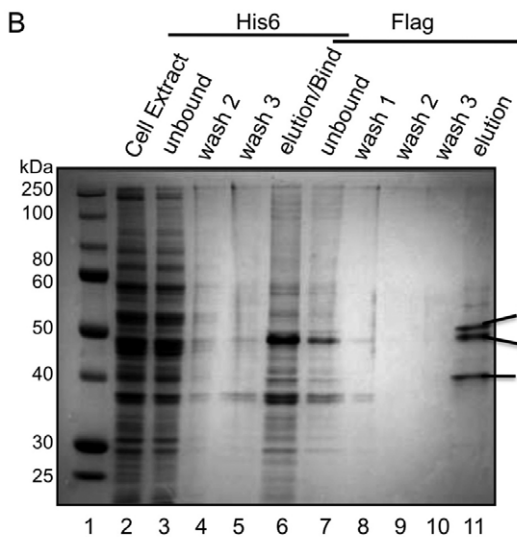
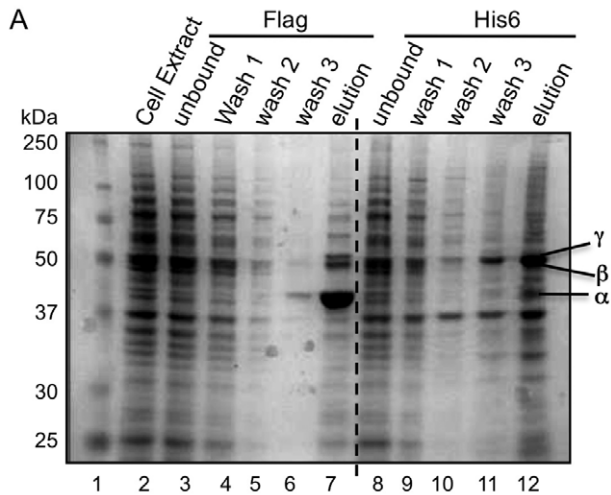


Figure 4. Purification of *heIF2*, *h2Bεcat* and GEF activity. A. and B.: Coomassie blue stained SDS-PAGE gel summaries of (A) single step partial-purification of *heIF2* from yeast strain GP6452 cell extracts (lane 2) using Flag M2 (lanes 3–7) or nickel agarose resins (lanes 8–12) or (B) sequential two-step purification of *heIF2* using first nickel agarose (lanes 3–6) and then Flag M2 affinity gel (lanes 7–11) that generated heterotrimeric eIF2. C. Left, coomassie blue stained SDS-PAGE gel of purified human eIF2 (labelled αβγ) and *h2Bεcat*. Right, GEF assays with wild type *h2Bεcat* or eIF2 alone. doi:10.1371/journal.pone.0053958.g004

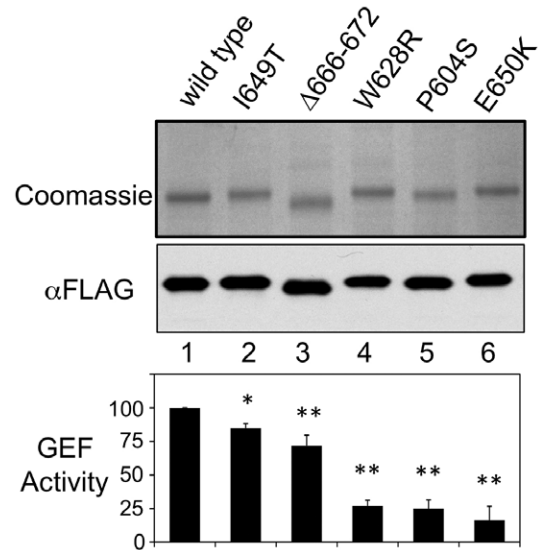


Figure 5. GEF activity of *h2Bεcat* CACH/WWM mutants. Top, purified eIF2B catalytic domains with indicated mutations both coomassie blue stained SDS-PAGE and Flag western blot are shown. Bottom: change in activity normalised to wild type (n = 4). 2 tailed T-test * $p < 0.05$, ** $p \leq 0.0001$. doi:10.1371/journal.pone.0053958.g005

eIF2B defects in immortalised lymphocytic cells compared to primary fibroblasts [51]. In summary, the recombinant *heIF2* performs as well as the previously used substrate in this assay and measurement of reduced GEF activity with *heIF2* and extracts from immortalised lymphocytic cells is diagnostic for eIF2B-mediated disease.

In conclusion, we describe a strategy for production of heterotrimeric recombinant human eIF2. We show that it can functionally replace yeast eIF2 *in vivo* and demonstrate its utility as a diagnostic tool for measuring the impact of eIF2B mutations that cause human disease. Employing recombinant *heIF2* from yeast will remove the need to use animal tissue sources to obtain purified eIF2 for these purposes.

Methods

Plasmid Constructions

Human eIF2 cDNA expression. Human cDNAs encoding *EIF2S1* (eIF2α) and *EIF2S2* (eIF2β) were cloned with N-terminal Flag or his6 epitope tags respectively into the pBEVY series of plasmids downstream of strong yeast promoters. These constructs failed to express any protein and on resequencing had acquired mutations within the promoter sequences. As the ORFs were intact, they were subcloned into pBEVY-GT, a multicopy yeast expression plasmid bearing divergent promoters from the *GAL1* and *GAL10* genes (P_{GAL1} and P_{GAL10}) that we have recently used with success elsewhere [52,53]. The cDNAs were cloned singly as Kpn1-EcoRI fragments downstream of P_{GAL1} creating pAV1901 (*EIF2S2*-his6) and pAV1907 (*EIF2S1*-Flag). In addition *EIF2S1*-Flag was cloned downstream of P_{GAL10} as a BamHI-Pst1 fragment in pAV1901 to create pAV1905 (*EIF2S2*-his6 and *EIF2S1*-Flag). *EIF2S3* (eIF2γ) cDNA was codon-optimized and synthesized (GeneScript USA Inc.) and subcloned as a Xba1-Sall fragment into pBEVY-GL creating pAV1970 and pBEVY-GU creating pAV1974. All constructs were confirmed by DNA sequence analysis. Further details are shown in Table 2.

Table 1. eIF2B GEF activities measured in extracts from lymphoblastoid cell lines from indicated CACH/VWM patents using *heIF2* and rat eIF2 substrates.

Patient Number	Mutated gene	Gene mutations (protein substitutions)	eIF2B GEF activity using <i>heIF2</i> (%)		eIF2B GEF activity using rat eIF2 (%)*		<i>heIF2</i> / rat eIF2
			Mean	SD	Mean	SD	
949-1	<i>EIF2B4</i>	c.728C>T/c.728C>T (Pro243Leu/Pro243Leu)	35.8	3.5	45.6	1.8	0.79
1036-1	<i>EIF2B5</i>	c.967C>T/c.1280C>T (Pro323Ser/Pro427Leu)	44.5	9.9	30	7.5	1.48
1838-1	<i>EIF2B4</i>	c.818T>C/c.1346C>T (Met273Thr/Thr449Ile)	44.5	2.1	46.8	6.4	0.95
1758-1	<i>EIF2B5</i>	c.338G>A/c.947G>A (Arg113His/Arg316Gln)	46.2	1.9	44.8	4.4	1.03
570-2	<i>EIF2B4</i>	c.626G>A/c.626G>A (Arg209Gln/Arg209Gln)	49.1	12.8	52	3	0.94
375-2	<i>EIF2B5</i>	c.338G>A/c.1948G>A (Arg113His/Glu650Leu)	56.2	3.1	59.4	0.7	0.95
1348-1	<i>EIF2B5</i>	c.338G>A/c.338G>A (Arg113His/Arg113His)	56.6	11.6	61.6	1.3	0.92
972-1	<i>EIF2B5</i>	c.943C>T/c.271A>G (Arg315Cys/Thr91Ala)	56.6	2.4	60.3	7	0.94
38	<i>EIF2B2</i>	c.638A>G/c.638A>G (Glu213Gly/Glu213Gly)	57.5	4	40.3	6.3	1.43
291-1 [§]	<i>EIF2B5</i>	c.338G>A/1160A>G (Arg113His/Asp387Gly)	58.6	17.7	41.5	6	1.41
1878-1	<i>EIF2B5</i>	c.338G>A/c.338G>A (Arg113His/Arg113His)	59.5	4.5	48.2	5.6	1.23
357-1	<i>EIF2B5</i>	c.406C>T/c.1015C>T (Arg136Cys/Arg339Trp)	63.7	17	44.5	4.5	1.43
571-1	<i>EIF2B5</i>	c.166T>G/c.944G>A (Phe56Val/Arg315His)	63.9	15.2	40	3	1.60
1963-1	<i>EIF2B5</i>	c.338G>A/c.338G>A (Arg113His/Arg113His)	64.4	14	69.2	4.3	0.93
1152-1	<i>EIF2B5</i>	c.134C>G/c.134C>G (Ala45Gly/Ala45Gly)	68	1.3	60.8	11.2	1.12
432-1	<i>EIF2B5</i>	c.338G>A/c.1884G>A (Arg113His/Trp628X)	86.4	12.4	90.4	1.8	1.04
1240-1	<i>EIF2B3</i>	c.604G>A/c.1312C>T (Ala202Thr/Arg438X)	87.2	26	67.7	2	1.29
1074-1	<i>EIF2B5</i>	c.338G>A/c.338G>A (Arg113His/Arg113His)	92	5.5	108	11.2	0.85

*Rat eIF2 data from [34].

SD standard deviation.

[§]patient previously reported as Arg113His/Arg113His in error [34].

doi:10.1371/journal.pone.0053958.t001

Human eIF2B ϵ catalytic domain. The *EIF2B5* (eIF2Be) catalytic domain (amino acids 533–721, termed here *h2B ϵ cat*) was identified by sequence alignment of translated ORF from Genbank (NG_015826) with the yeast *Saccharomyces cerevisiae* Gcd6p catalytic domain [32,33]. The cDNA was codon optimised and custom synthesized (GeneScript USA Inc) with the 3'UTR of *GCD6*. This was subcloned using MluI and BamHI into plasmid pAV1427 in frame with 5' tandem Flag and his₆ tags downstream of the *P_{GAL1}* promoter creating plasmid pAV2075. Quikchange (Agilent) site-directed mutagenesis kit was used to introduce mutations into the GeneScript clone prior to subcloning into pAV1427 to create the plasmids pAV2095-99, each identical to pAV1075 except for the site-directed changes shown in Table 2. All constructs were confirmed by DNA sequence analysis.

Yeast (*S. cerevisiae*) Genetic Methods

All constructions employed standard methods and yeast media [54]. Transformations used the lithium acetate method. For serial dilution growth assays cells were grown in YPGal liquid medium (2% galactose, 2% raffinose) to logarithmic phase, diluted to A₆₀₀ = 0.1 and 10-fold serially diluted. 2 μ l of each dilution was spotted on solid medium and plates were incubated at 30°C. Deletion of *TRP1* in GP5010 and GP5012 (see Table 3) used plasmid pNKY1009 (*trp1 Δ ::hisG-URA3-hisG*) [55]. The *trp1 Δ ::loxP-hphNT1-loxP* was introduced into GP6124 by PCR amplification using pZC1(pAV2170) [56] as template to disrupt *TRP1* with the *loxP-hphNT1-loxP* cassette. Plasmid shuffling employed 5-fluoroorotic acid (FOA) [54]. When shuffling plasmids requiring *P_{GAL}* expression, cells were grown in YPGal medium prior to shuffling,

and FOA medium used 2% galactose in place of glucose. All strains used are summarized in Table 3.

To assess complementation of the slow-growth phenotype of strains expressing *EIF2S3* as the sole source of eIF2 γ , strains GP5613 or GP5614 were transformed with the following high copy plasmids to alter the levels of the indicated factors: tRNA^{Met} pAV1345 (*IMT4 LEU2*); eIF2B pAV1428 (*GCD1 GCD6 URA3*) and pAV1494 (*GCD2 GCD7 GCN3 LEU2*); eIF5 pAV2015 (*TIF5 URA3*); eIF3 pAV2112 (*TIF31 NIP1 LEU2*) and pAV2113 (*PRT1 TIF35 TIF34 HCR1 URA3*). Only excess eIF5 reproducibly suppressed the slow-growth phenotype. In some experiments other slow-growth suppressing colonies were obtained, but not reproducibly. Except for eIF5, we assume that suppression was caused by altered *EIF2S3* expression similar to that shown in Figure 2A, rather than true suppressive effects of the transformed plasmid. In addition, combinations of overexpressed eIF2 subunits were assessed: pAV1346 (*SUI2 SUI3 URA3*) pAV1348 (*GCD11 SUI2 SUI3 URA3*) or the low copy plasmid pAV1280 (*GCD11 CEN*). Only plasmids bearing *GCD11* suppressed slow-growth.

Protein Purification

eIF2. Strain GP6452 contains plasmids for galactose induced expression of human eIF2 (*heIF2*) (Table 3). 20 litres SCGal medium containing 2% Galactose +2% Raffinose +0.25% Glucose carbon sources and lacking leucine, tryptophan and uracil was grown to A₆₀₀ ~5 in 5 litre flasks. Cells (~80 g wet weight) were harvested by centrifugation (6000 rpm, 15 mins Beckman JLA8.1000 rotor), washed in ice-cold water and resuspended at 2 ml/g in lysis buffer [100 mM Tris/HCl (pH 8), 500 mM KCl,

Table 2. Plasmids used or constructed for this study.

Designation	Genes	Source/Construction summary
pAV1228	<i>SUI3 LEU2 CEN4</i>	A. Hinnebusch p920
pAV1255	<i>SUI2 LEU2 CEN4</i>	A. Hinnebusch p1097
pAV1280	<i>GCD11 URA3 CEN4</i>	E. Hannig Ep293
pAV1345	<i>IMT4 LEU2 2μm</i>	A. Hinnebusch p1775 [58]
pAV1346	<i>SUI2 SUI3 URA3 2μm</i>	A. Hinnebusch p1778 [58]
pAV1348	<i>GCD11 SUI2 SUI3 URA3 2μm</i>	A. Hinnebusch p1780 [58]
pAV1427	<i>P_{GAL1}Flag-His₆-GCD6 URA3 leu2d 2μm</i>	[59]
pAV1428	<i>GCD1-Flag₂-His₆ GCD6 URA3 2μm</i>	[59]
pAV1494	<i>GCD2 GCD7 GCN3 LEU2 2μm</i>	[59]
pAV1702	<i>P_{GAL1} P_{GAL10} 2μm LEU2</i>	pBEVY-GL dual promoter galactose expression vector [52]
pAV1703	<i>P_{GAL1} P_{GAL10} 2μm TRP1</i>	pBEVY-GT dual promoter galactose expression vector [52]
pAV1704	<i>P_{GAL1} P_{GAL10} 2μm URA3</i>	pBEVY-GU dual promoter galactose expression vector [52]
pAV1874	<i>TRP1 P_{GPD}EIF2S1-Flag P_{ADH1}EIF2S2-His₆ 2μm</i>	Epitope tagged human cDNAs amplified and cloned in pBEVY-T Note-Promoter mutations prevent expression.
pAV1901	<i>TRP1 P_{GAL1}EIF2S2-His₆ 2μm</i>	human <i>EIF2S2</i> -His ₆ digested from pAV1874 (KpnI/EcoRI) and ligated into pAV1703
pAV1905	<i>TRP1 P_{GAL10}EIF2S1-Flag P_{GAL1}His₆-EIF2S2 2μm</i>	human <i>EIF2S1</i> -Flag from pAV1874 (BamHI/PstI) ligated into pAV1901
pAV1907	<i>P_{GAL1}EIF2S1-Flag 2μm TRP1</i>	human <i>EIF2S1</i> -Flag KpnI/EcoRI digested from pAV1874 and ligated into pAV1703
pAV1970	<i>P_{GAL10}EIF2S3 2μm LEU2</i>	Codon optimised <i>EIF2S3</i> cloned into pAV1704 by XbaI/Sall digestion and ligation.
pAV1974	<i>P_{GAL10}EIF2S3 2μm URA3</i>	Codon optimised <i>EIF2S3</i> cloned into pAV1702 by XbaI/Sall digestion and ligation.
pAV2015	<i>TIF5-Flag URA3 2μm</i>	K. Asano KAB446
pAV2075	<i>URA3 P_{GAL1}Flag-His₆-EIF2B5cat leu2d 2μm</i>	Codon optimised commercially synthesized human <i>EIF2B5</i> cDNA (codons 533–721 only) cloned MluI/BamHI into pAV1427 removing <i>GCD6</i> .
pAV2095	<i>URA3 P_{GAL1}Flag-His₆-EIF2B5cat-I649T leu2d 2μm</i>	Site directed mutagenesis introduced mutation into <i>EIF2B5</i> (533–721) cDNA as described for pAV2075.
pAV2096	<i>P_{GAL1}Flag-His₆-EIF2B5cat-Δ664–671 URA3 leu2d 2μm</i>	Site directed mutagenesis as above
pAV2097	<i>P_{GAL1}Flag-His₆-EIF2B5cat-W628R URA3 leu2d 2μm</i>	Site directed mutagenesis as above
pAV2098	<i>P_{GAL1}Flag-His₆-EIF2B5cat-P604S URA3 leu2d 2μm</i>	Site directed mutagenesis as above
pAV2099	<i>P_{GAL1}Flag-His₆-EIF2B5cat-E650K URA3 leu2d 2μm</i>	Site directed mutagenesis as above
pAV2112	<i>TIF32 NIP1-His₆ LEU2 2μm</i>	L. Valasek, Prague
pAV2113	<i>PRT1 TIF35 TIF34 HCR1 URA3 2μm</i>	L. Valasek, Prague

doi:10.1371/journal.pone.0053958.t002

5 mM MgCl₂, 5 mM NaF, 10 mM Imidazole, 7 mM 2-mercaptoethanol, 10% Glycerol, 0.1% Triton X100, protease inhibitor tablet (Roche) and 1 μ g/ml pepstatin, 1 μ g/ml leupeptin and 1 μ g/ml aprotinin and frozen under liquid nitrogen. Cells were lysed using a large cryogenic freezer mill (Spex Certiprep Ltd) and stored at -80°C prior to purification. All subsequent steps were performed at 4°C . Cells were thawed and cell debris removed by centrifugation at 5000 *g* (Sigma 4K15 centrifuge) and the resulting extract was clarified by successive rounds of centrifugation at 22,000 *g*, 30 min, (Heraeus Biofuge Stratos) and 440,000 *g*, 1 hr, (Beckman ultracentrifuge Ti70.1 rotor). Nickel affinity chromatography (Qiagen) was performed in batch mode with rotation for 2 hrs. Resin was collected by low speed centrifugation (2000 rpm), washed four times with Ni Wash buffer (as Lysis buffer, but with 100 mM KCl, 25 mM Imidazole) and eluted (2 \times 1 hr) in Ni Elution buffer (as Ni Wash buffer, but with 500 mM Imidazole). Elutions were combined and dialysed against Flag Wash buffer (as Ni Wash buffer but lacking imidazole), then mixed with 1 ml prewashed Flag M2 agarose resin (Sigma) in batch binding mode for 2 hours. Following three

washes in Flag Wash buffer, protein elutions were performed (2 \times 30 min) in Flag Elution buffer [Flag Wash buffer with 0.4 mg/ml 3X Flag peptide (Sigma)]. Finally purified samples were dialysed into storage buffer [30 mM HEPES (pH7.5), 100 mM KCl, 1 mM DTT, 0.1 mM EDTA, 10% glycerol, 0.1% Igepal CA-630] then aliquoted and stored at -80°C . Typically a yield of 2.4 mg eIF2 was purified (Micro-BCA assay, Pierce).

eIF2B ϵ catalytic domain. Strain GP5548 contains plasmid pAV2075 for yeast expression codon-optimized galactose-induced expression of Flag and his₆ tandem tagged *h2B ϵ cat*. Strains GP5644-5648 similarly express specific mutant forms of the same protein (Table 3). Our purification scheme was performed as described for human eIF2, except on a smaller scale starting with 8–20 g wet weight cell pellet. Typically 300–500 μ g was purified from 20 g starting cell pellet.

Western Blotting

Extracts from exponentially growing yeast cells were made using glass beads and a FastPrep-24 (MP Biomedicals). Typically

Table 3. Yeast Strains Used in this study.

Designation	Genotype	Source/reference
GP3001	<i>MATa leu2-3 leu2-112 sui2Δ trp1-Δ63 ura3-52 [SUI2 CEN LEU2]</i>	Pavitt collection
GP3582	<i>MATa gcd11Δ::hisG leu2-3 leu2-112 ino1 ura3-52::HIS4-lacZ [URA3 CEN GCD11]</i>	Pavitt collection, (A. Hinnebusch NIH -F484)
GP3889	<i>MATα gcn2Δ leu2-3 leu2-112 pep4::LEU2 trp1-Δ63 ura3-52</i>	Pavitt collection
GP4907	<i>MATα gcn2Δ leu2-3 leu2-112 ino1 sui3Δ HIS4-lacZ::ura3-52 [SUI3 CEN LEU2]</i>	K. Asano, KAY17
GP5010	<i>trp1Δ::hisG</i> in GP4907	This Study
GP5012	<i>trp1Δ::hisG</i> in GP3582	This Study
GP5108	[<i>P_{GAL10}EIF2S1-Flag 2μm TRP1</i>] plasmid shuffle in GP3001	This Study
GP5109	[<i>P_{GAL10}EIF2S1-Flag P_{GAL1}EIF2S2-His6 2μm TRP1</i>] plasmid shuffle in GP3001	This Study
GP5110	[<i>P_{GAL1}EIF2S2-His6 2μm TRP1</i>] plasmid shuffle in GP5010	This Study
GP5111	[<i>P_{GAL10}EIF2S1-Flag P_{GAL1} EIF2S2-His6 2μm TRP1</i>] plasmid shuffle in GP5010	This Study
GP5548	GP3889 [<i>P_{GAL1}Flag-His6-EIF2B5cat URA3 leu2d 2μm</i>]	This Study
GP5613	[<i>P_{GAL10}EIF2S3 2μm LEU2</i>] FOA plasmid shuffle in GP5012	This Study
GP5614	[<i>P_{GAL10}EIF2S3 2μm TRP1</i>] FOA plasmid shuffle in GP5012	This Study
GP5644	GP3889 [<i>P_{GAL1}-Flag-His6-EIF2B5cat-I649T URA3 leu2d 2μm</i>]	This Study
GP5645	GP3889 [<i>P_{GAL1}-Flag-His6-EIF2B5cat-Δ664-671 URA3 leu2d 2μm</i>]	This Study
GP5646	GP3889 [<i>P_{GAL1}-Flag-His6-EIF2B5cat-W628R URA3 leu2d 2μm</i>]	This Study
GP5647	GP3889 [<i>P_{GAL1}-Flag-His6-EIF2B5cat-P604S URA3 leu2d 2μm</i>]	This Study
GP5648	GP3889 [<i>P_{GAL1}-Flag-His6-EIF2B5cat-E650K URA3 leu2d 2μm</i>]	This Study
GP5744	GP5613 [<i>URA3 2μm</i>]	This Study
GP5755	GP5613 [<i>GCD11 CEN URA3</i>]	This Study
GP5758	GP5613 [<i>TIF5 2μm URA3</i>]	This Study
GP6122	<i>MATa gcd11Δ::Nat gcn2Δ::hisG his3Δ0 leu2Δ0 met15Δ0 pep4::HIS3 sui2Δ::hisG sui3Δ::KanMX ura3Δ0 [GCD11 SUI2 SUI3 URA3 2μm]</i>	T. Dever J551 [43]
GP6124	<i>trp1Δ::hphNT1</i> in GP6122	This Study
GP6452	GP3889 [<i>P_{GAL10}EIF2S3 2μm LEU2</i>] [<i>P_{GAL10}EIF2S1-Flag P_{GAL1}EIF2S2-His6 2μm TRP1</i>] [<i>P_{GAL10}EIF2S3 2μm URA3</i>]	This Study
GP6461	[<i>P_{GAL10}EIF2S3 2μm LEU2</i>] [<i>P_{GAL10}EIF2S1-Flag P_{GAL1}EIF2S2-His6 2μm TRP1</i>] FOA plasmid shuffle in GP6124 (#1)	This Study
GP6462	[<i>P_{GAL10}EIF2S3 2μm LEU2</i>] [<i>P_{GAL10}EIF2S1-Flag P_{GAL1}EIF2S2-His6 2μm TRP1</i>] FOA plasmid shuffle in GP6124 (#2)	This Study

doi:10.1371/journal.pone.0053958.t003

8×A₆₀₀ units of cells were washed and resuspended in 200 μl Laemmli sample buffer, processed for 5×30 seconds at 6 ms⁻¹ setting in the FastPrep-24 at 4°C. 20 μl of each sample was resolved on 10 or 12% acrylamide SDS-PAGE, transferred to nitrocellulose membranes and probed with antibodies: Flag M2 (Sigma, 1:500), His6 (BD Biosciences 51.9000012, 1:1000) eIF2γ (Abcam AB33207, 1:1000), Gcd11p (1:5000; E. Hannig, Texas), Tif5p (1:1000) [57], Tsa1p (Abcam AB33207, 1:1000; the human eIF2γ antibody was raised to an epitope shared with yeast Tsa1p: epitope TIKPTVDDD; Tsa1p TIKPTVeDs), Sui2p (1:1000; T. Dever, NIH), Sui3p (1:500) [50]. HRP conjugated secondary antibodies (Abcam) and enhanced chemiluminescence detection system (Pierce) were used.

GEF Assays

eIF2B GEF activity measured with purified h2Bεcat. Activity was measured using a standard filter binding assay with eIF2 and radiolabelled GDP. eIF2•[³H]GDP binary complexes were formed in binary complex buffer [30 mM HEPES (pH 7.5), 100 mM KCl, 0.1 mM EDTA, 1 mg/ml BSA, 1 mM DTT] with 30 pmol eIF2 and 0.5 μCi [³H]GDP (4.5 Ci mmol⁻¹) at 20°C for 10 min and stabilized by the addition of 1 mM MgCl₂. Nucleotide exchange was initiated by the addition of 2 μg h2Bεcat and unlabelled GDP (2 nmol). Samples were removed at regular

intervals and filtered through nitrocellulose filters, dried and counted by liquid scintillation.

eIF2B GEF activity measured in patients cell extracts. An Institutional Review Board of the participating centers (Comité de Protection des Personnes Sud-Est VI, 2009-A00188-49) approved the use of human subjects for this study. A written informed consent was obtained from all patients [34].

Activity measured with extracts from patient lymphoblastoid cell lines (lymphoblasts) as a source of eIF2B was performed with hEIF2 as described previously for eIF2 purified from rat liver [7,25] with the following modifications: the use of 1 μCi [³H]GDP (4.5 Ci mmol⁻¹) for eIF2•[³H]GDP binary complex formation, incubation of this mixture at 30°C for 30 min (instead of 10 min), and the [³H]GDP dissociation kinetics was monitored every 5 min (instead of every 2 min: from 0 to 15 min). Such comparative analyses were performed at least in triplicate for cells from 18 patients and matched controls.

Acknowledgments

We acknowledge Ahmed Abd El Maksoud (Manchester) for assistance in construction of pAV2095-2099, K. Asano (Kansas) for the *SUI3* deletion strain, Thomas Dever (NIH) for the eIF2 triple deletion yeast strain, and Leos Valasek (Prague) for plasmids overexpressing subunits of yeast eIF3.

We also thank Mark Ashe, Chris Grant and other members of the Pavitt laboratory for helpful discussions during the course of this work.

References

- Schiffmann R, Moller JR, Trapp BD, Shih HH, Farrer RG, et al. (1994) Childhood ataxia with diffuse central nervous system hypomyelination. *Ann Neurol* 35: 331–340.
- van der Knaap MS, Barth PG, Gabreels FJ, Franzoni E, Begeer JH, et al. (1997) A new leukoencephalopathy with vanishing white matter. *Neurology* 48: 845–855.
- Fogli A, Boespflug-Tanguy O (2006) The large spectrum of eIF2B-related diseases. *Biochem Soc Trans* 34: 22–29.
- Pavitt GD, Proud CG (2009) Protein synthesis and its control in neuronal cells with a focus on vanishing white matter disease. *Biochem Soc Trans* 37: 1298–1310.
- Leegwater PA, Vermeulen G, Konst AA, Naidu S, Mulders J, et al. (2001) Subunits of the translation initiation factor eIF2B are mutant in leukoencephalopathy with vanishing white matter. *Nat Genet* 29: 383–388.
- Labauge P, Horzinski L, Avyrnac X, Blanc P, Vukusic S, et al. (2009) Natural history of adult-onset eIF2B-related disorders: a multi-centric survey of 16 cases. *Brain* 132: 2161–2169.
- Richardson JP, Mohammad SS, Pavitt GD (2004) Mutations causing childhood ataxia with central nervous system hypomyelination reduce eukaryotic initiation factor 2B complex formation and activity. *Mol Cell Biol* 24: 2352–2363.
- Li W, Wang X, Van Der Knaap MS, Proud CG (2004) Mutations linked to leukoencephalopathy with vanishing white matter impair the function of the eukaryotic initiation factor 2B complex in diverse ways. *Mol Cell Biol* 24: 3295–3306.
- Leng X, Wu Y, Wang X, Pan Y, Wang J, et al. (2011) Functional analysis of recently identified mutations in eukaryotic translation initiation factor 2B epsilon (eIF2Bε) identified in Chinese patients with vanishing white matter disease. *J Hum Genet* 56: 300–305.
- Fogli A, Schiffmann R, Hugendubler L, Combes P, Bertini E, et al. (2004) Decreased guanine nucleotide exchange factor activity in eIF2B-mutated patients. *Eur J Hum Genet* 12: 561–566.
- Vanderver A, Schiffmann R, Timmons M, Kellersberger KA, Fabris D, et al. (2005) Decreased asialotransferrin in cerebrospinal fluid of patients with childhood-onset ataxia and central nervous system hypomyelination/vanishing white matter disease. *Clin Chem* 51: 2031–2042.
- Wong K, Armstrong RC, Gyure KA, Morrison AL, Rodriguez D, et al. (2000) Foamy cells with oligodendroglial phenotype in childhood ataxia with diffuse central nervous system hypomyelination syndrome. *Acta Neuropathol (Berl)* 100: 635–646.
- Dietrich J, Lacagnina M, Gass D, Richfield E, Mayer-Proschel M, et al. (2005) EIF2B5 mutations compromise GFAP+ astrocyte generation in vanishing white matter leukodystrophy. *Nat Med* 11: 277–283.
- van Kollenburg B, van Dijk J, Garbern J, Thomas AA, Scheper GC, et al. (2006) Glia-specific activation of all pathways of the unfolded protein response in vanishing white matter disease. *J Neuropathol Exp Neurol* 65: 707–715.
- Bugiani M, Boor I, van Kollenburg B, Postma N, Polder E, et al. (2011) Defective glial maturation in vanishing white matter disease. *J Neuropathol Exp Neurol* 70: 69–82.
- Fogli A, Merle C, Roussel V, Schiffmann R, Ughetto S, et al. (2012) CSF N-Glycan Profiles to Investigate Biomarkers in Brain Developmental Disorders: Application to Leukodystrophies Related to eIF2B Mutations. *PLoS One* 7: e42688.
- Geva M, Cabilly Y, Assaf Y, Mindroul N, Marom L, et al. (2010) A mouse model for eukaryotic translation initiation factor 2B-leukodystrophy reveals abnormal development of brain white matter. *Brain* 133: 2448–2461.
- Huyghe A, Horzinski L, Henaut A, Gaillard M, Bertini E, et al. (2012) Developmental splicing deregulation in leukodystrophies related to EIF2B mutations. *PLoS One* 7: e38264.
- Pavitt GD (2005) eIF2B, a mediator of general and gene-specific translational control. *Biochem Soc Trans* 33: 1487–1492.
- Lorsch JR, Dever TE (2010) Molecular view of 43 S complex formation and start site selection in eukaryotic translation initiation. *J Biol Chem* 285: 21203–21207.
- Hinnebusch AG (2011) Molecular mechanism of scanning and start codon selection in eukaryotes. *Microbiol Mol Biol Rev* 75: 434–467.
- Sonenberg N, Hinnebusch AG (2009) Regulation of translation initiation in eukaryotes: mechanisms and biological targets. *Cell* 136: 731–745.
- Pavitt GD, Yang W, Hinnebusch AG (1997) Homologous segments in three subunits of the guanine nucleotide exchange factor eIF2B mediate translational regulation by phosphorylation of eIF2. *Mol Cell Biol* 17: 1298–1313.
- Kimball SR, Fabian JR, Pavitt GD, Hinnebusch AG, Jefferson LS (1998) Regulation of guanine nucleotide exchange through phosphorylation of eukaryotic initiation factor eIF2α. Role of the alpha- and delta- subunits of eIF2B. *J Biol Chem* 273: 12841–12845.
- Elsby R, Heiber JF, Reid P, Kimball SR, Pavitt GD, et al. (2011) The alpha subunit of eukaryotic initiation factor 2B (eIF2B) is required for eIF2-mediated translational suppression of vesicular stomatitis virus. *J Virol* 85: 9716–9725.
- Goss DJ, Parkhurst IJ, Mehta HB, Woodley CL, Wahba AJ (1984) Studies on the role of eukaryotic nucleotide exchange factor in polypeptide chain initiation. *J Biol Chem* 259: 7374–7377.
- Kimball SR, Everson WV, Myers LM, Jefferson LS (1987) Purification and characterization of eukaryotic initiation factor 2 and a guanine nucleotide exchange factor from rat liver. *J Biol Chem* 262: 2220–2227.
- Oldfield S, Proud CG (1992) Purification, phosphorylation and control of the guanine-nucleotide-exchange factor from rabbit reticulocyte lysates. *Eur J Biochem* 208: 73–81.
- Pavitt GD, Ramaiah KV, Kimball SR, Hinnebusch AG (1998) eIF2 independently binds two distinct eIF2B subcomplexes that catalyze and regulate guanine-nucleotide exchange. *Genes Dev* 12: 514–526.
- Williams DD, Pavitt GD, Proud CG (2001) Characterization of the initiation factor eIF2B and its regulation in *Drosophila melanogaster*. *J Biol Chem* 276: 3733–3742.
- Fabian JR, Kimball SR, Heinzinger NK, Jefferson LS (1997) Subunit assembly and guanine nucleotide exchange activity of eukaryotic initiation factor-2B expressed in Sf9 cells. *J Biol Chem* 272: 12359–12365.
- Gomez E, Mohammad SS, Pavitt GD (2002) Characterization of the minimal catalytic domain within eIF2B: the guanine-nucleotide exchange factor for translation initiation. *EMBO J* 21: 5292–5301.
- Boesen T, Mohammad SS, Pavitt GD, Andersen GR (2004) Structure of the catalytic fragment of translation initiation factor 2B and identification of a critically important catalytic residue. *J Biol Chem* 279: 10584–10592.
- Horzinski L, Huyghe A, Cardoso MC, Gonthier C, Ouchchane L, et al. (2009) Eukaryotic initiation factor 2B (eIF2B) GEF activity as a diagnostic tool for EIF2B-related disorders. *PLoS One* 4: e8318.
- Erickson FL, Hannig EM (1996) Ligand interactions with eukaryotic translation initiation factor 2: role of the γ-subunit. *EMBO J* 15: 6311–6320.
- Asano K, Krishnamoorthy T, Phan L, Pavitt GD, Hinnebusch AG (1999) Conserved bipartite motifs in yeast eIF5 and eIF2Bepsilon, GTPase-activating and GDP-GTP exchange factors in translation initiation, mediate binding to their common substrate eIF2. *EMBO J* 18: 1673–1688.
- Valasek L, Nielsen KH, Hinnebusch AG (2002) Direct eIF2-eIF3 contact in the multifactor complex is important for translation initiation in vivo. *EMBO J* 21: 5886–5898.
- Schmitt E, Naveau M, Mechulam Y (2010) Eukaryotic and archaeal translation initiation factor 2: a heterotrimeric tRNA carrier. *FEBS Lett* 584: 405–412.
- Asano K, Clayton J, Shalev A, Hinnebusch AG (2000) A multifactor complex of eukaryotic initiation factors, eIF1, eIF2, eIF3, eIF5, and initiator tRNA(Met) is an important translation initiation intermediate in vivo. *Genes Dev* 14: 2534–2546.
- Singh CR, Lee B, Udagawa T, Mohammad-Qureshi SS, Yamamoto Y, et al. (2006) An eIF5/eIF2 complex antagonizes guanine nucleotide exchange by eIF2B during translation initiation. *EMBO J* 25: 4537–4546.
- Singh CR, Udagawa T, Lee B, Wassink S, He H, et al. (2007) Change in nutritional status modulates the abundance of critical pre-initiation intermediate complexes during translation initiation in vivo. *J Mol Biol* 370: 315–330.
- Jennings MD, Pavitt GD (2010) eIF5 is a dual function GAP and GDI for eukaryotic translational control. *Small Gtpases* 1: 118–123.
- Shin BS, Kim JR, Walker SE, Dong J, Lorsch JR, et al. (2011) Initiation factor eIF2γ promotes eIF2-GTP-Met-tRNAi(Met) ternary complex binding to the 40S ribosome. *Nat Struct Mol Biol* 18: 1227–1234.
- Wei J, Jia M, Zhang C, Wang M, Gao F, et al. (2010) Crystal structure of the C-terminal domain of the varespin subunit of human translation initiation factor eIF2B. *Protein Cell* 1: 595–603.
- Kaczorowska M, Kuczynski D, Jurkiewicz E, Scheper GC, van der Knaap MS, et al. (2006) Acute fright induces onset of symptoms in vanishing white matter disease-case report. *Eur J Paediatr Neurol* 10: 192–193.
- Pronk JC, van Kollenburg B, Scheper GC, van der Knaap MS (2006) Vanishing white matter disease: a review with focus on its genetics. *Ment Retard Dev Disabil Res Rev* 12: 123–128.
- Fogli A, Schiffmann R, Bertini E, Ughetto S, Combes P, et al. (2004) The effect of genotype on the natural history of eIF2B-related leukodystrophies. *Neurology* 62: 1509–1517.
- van der Lei HD, van Berkel CG, van Wieringen WN, Brenner C, Feigenbaum A, et al. (2010) Genotype-phenotype correlation in vanishing white matter disease. *Neurology* 75: 1555–1559.
- Liu AR, van der Lei HD, Wang X, Wortham NC, Tang H, et al. (2011) Severity of Vanishing White Matter disease does not correlate with deficits in eIF2B activity or the integrity of eIF2B complexes. *Hum Mutat*.

Author Contributions

Conceived and designed the experiments: GDP GCS OBT. Performed the experiments: RAA AF MG. Analyzed the data: RAA AF GDP. Contributed reagents/materials/analysis tools: GCS OBT GDP. Wrote the paper: GDP AF OBT RAA GCS.

50. Mohammad-Qureshi SS, Haddad R, Hemingway EJ, Richardson JP, Pavitt GD (2007) Critical contacts between the eukaryotic initiation factor 2B (eIF2B) catalytic domain and both eIF2beta and -2gamma mediate guanine nucleotide exchange. *Mol Cell Biol* 27: 5225–5234.
51. Horzinski L, Kantor L, Huyghe A, Schiffmann R, Elroy-Stein O, et al. (2010) Evaluation of the endoplasmic reticulum-stress response in eIF2B-mutated lymphocytes and lymphoblasts from CACH/VWM patients. *BMC Neurol* 10: 94.
52. Miller CA, 3rd, Martinat MA, Hyman LE (1998) Assessment of aryl hydrocarbon receptor complex interactions using pBEVY plasmids: expression-vectors with bi-directional promoters for use in *Saccharomyces cerevisiae*. *Nucleic Acids Res* 26: 3577–3583.
53. Reid PJ, Mohammad-Qureshi SS, Pavitt GD (2012) Identification of intersubunit domain interactions within eukaryotic initiation factor (eIF) 2B, the nucleotide exchange factor for translation initiation. *J Biol Chem* 287: 8275–8285.
54. Adams A, Gottschling DE, Kaiser CA, Stearns T (1998) *Methods in Yeast genetics: A Cold Spring Harbor Laboratory Course Manual*. Cold Spring Harbor, NY: Cold Spring Harbor Laboratory Press. 177 p.
55. Alani E, Cao L, Kleckner N (1987) A method for gene disruption that allows repeated use of URA3 selection in the construction of multiply disrupted yeast strains. *Genetics* 116: 541–545.
56. Carter Z, Delneri D (2010) New generation of loxP-mutated deletion cassettes for the genetic manipulation of yeast natural isolates. *Yeast* 27: 765–775.
57. Jennings MD, Pavitt GD (2010) eIF5 has GDI activity necessary for translational control by eIF2 phosphorylation. *Nature* 465: 378–381.
58. Dever TE, Yang W, Astrom S, Bystrom AS, Hinnebusch AG (1995) Modulation of tRNA^{Met}, eIF-2 and eIF-2B expression shows that *GCN4* translation is inversely coupled to the level of eIF-2-GTPMet-tRNA^{Met} ternary complexes. *Mol Cell Biol* 15: 6351–6363.
59. Gomez E, Pavitt GD (2000) Identification of domains and residues within the epsilon subunit of eukaryotic translation initiation factor 2B (eIF2Bepsilon) required for guanine nucleotide exchange reveals a novel activation function promoted by eIF2B complex formation. *Mol Cell Biol* 20: 3965–3976.